Proceedings of the 2025 SICE Festival with Annual Conference
September 9-12, 2025, Chiang Mai, Thailand

Measurement of Shear Stress Induced by Supersonic Jet Impingement

Yo Murata[1†] and Masaki Endo[2]

[1] Mechanical Engineering, Tokyo Denki University, Saitama, Japan
(E-mail: 25udm05@ms.dendai.ac.jp)
[2] Division of Mechanical Engineering, Tokyo Denki University, Saitama, Japan
(E-mail: mendo@mail.dendai.ac.jp)

Abstract: When the fluid flows around an object, the viscosity induces the shear stress on its surface, which is an important physical quantity in fields like aerospace, automotive, and laser processing. Oil-Film Interferometry (OFI) is a non-intrusive technique that visualizes and quantifies this shear stress. In this study, the shear stress due to supersonic jet impingement on a flat plate was measured using OFI. The spacing of the interference fringes was measured with respect to the elapsed time, revealing that shear stress was inversely proportional to distance from the jet impingement point.

Keywords: Oil-Film Interferometry, Fluid Friction, Turbulent Flow, Interference Fringes.

1. INTRODUCTION

Accurate measurement of the shear stress acting on the surface of an object due to fluid flow has been recognized as a critically important issue in the field of practical engineering. In particular, the aerospace, maritime, and automotive industries are faced with the need to reduce fossil fuel consumption through energy conservation and efficient energy use. Accurate and precise measurement of the shear stress is essential to achieve higher energy efficiency by reducing frictional drag.

Furthermore, the shear stress measurement also plays a crucial role in evaluating the performance of air dusters and the capability of removing molten metal during laser processing. The air dusters have long been used in metalworking processes, and various nozzles have been proposed by many companies to improve their efficiency. However, there is no defined index to indicate the removal capacity of cutting debris, and each company uses its own method to evaluate the performance. In laser processing, there is a growing demand for processing thicker plates. There is also a need to clarify the appropriate values for nozzle position relative to the work piece and supply pressure for efficient removal of molten metal.

Various shear stress measurement techniques have been proposed to date, some of which have been practically applied in engineering fields. Among these, Oil-Film Interferometry (OFI), proposed by Tanner and Blows, is widely recognized as a representative method because it causes very little disturbance to the flow field. OFI also has the advantage of requiring a relatively simple experimental setup, and it is expected to be used in practical applications in the engineering field.

In this method, a thin oil film of less than 10 μm thickness is spread over the surface of an object. When the film is irradiated with monochromatic light, interference fringes are observed, allowing visualization of the thinning process caused by the shear stress of fluid flow passing over the surface. As the oil film becomes thinner over time, the spacing between adjacent dark fringes increases. Since the rate of this spacing expansion is proportional to the shear stress, its quantitative evaluation is possible [1]. OFI is applicable over a wide Mach number range and has been used for measuring shear stress on the surface of aircraft wings [2].

In the present study, an experiment was conducted for a supersonic jet impinging on a flat plate. The jet spreads radially over the plate, and then the wall jet is formed. The distribution of shear stress generated by the wall jet was measured using OFI.

2. METHODOLOGY

Since the thickness of an oil film spreading over a flat plate has a wedge-shaped distribution, illuminating the film with monochromatic light causes interference fringes to appear due to optical path differences. OFI is a method that utilizes these interference fringes to measure shear stress from the thickness of the oil. When oil is dropped onto a flat plate and air is blown along the surface, the frictional force between the air and the oil surface causes the oil to spread, and the spacing of the fringes gradually increases. This change is captured through interval photography, and shear stress is calculated from the velocity of fringe movement.

Fig. 1 shows the optical path difference in the film. The light reflected at the oil surface and the light transmitted through the oil and reflected at the plate surface interfere with each other, resulting in alternating bright and dark lines. According to Snell's law, the refraction angle β in the oil film is given by the following equation.

$$\sin\beta = \frac{\sin\alpha}{n_{\mathrm{oil}}} \tag{1}$$

where n_{oil} is the refractive index of the oil and α is the incident angle of the light. From geometric relations and Eq. (1), cosβ is expressed as follows:

$$\cos\beta = \sqrt{1 - \sin^2\beta} = \frac{\sqrt{n_{\mathrm{oil}}^2 - \sin^2\alpha}}{n_{\mathrm{oil}}} \tag{2}$$

† Yo Murata is the presenter of this paper.

Assuming the optical path difference between adjacent fringes equals the wavelength λ_0 of the light, the following equation is obtained.

$$2n_{\mathrm{oil}}\,\Delta h\cos\beta = \lambda_0 \tag{3}$$

where Δh is the difference in oil film thickness. Solving for Δh and substituting equation (2) gives the following expression for the thickness difference between adjacent dark fringes.

$$\Delta h = \frac{\lambda_0}{2\sqrt{n_{\mathrm{oil}}^2 - \sin^2\alpha}} \tag{4}$$

Assuming the oil is a Newtonian fluid, according to Newton's law of viscosity, the shear stress τ at height y from the flat plate and velocity u of the oil is given by

$$\tau = \mu\frac{du}{dy} = \rho\nu\frac{du}{dy} \tag{5}$$

where ρ is the density and ν is the kinematic viscosity of the oil. If the shear stress is constant in the flow direction, the velocity gradient is also constant as follows:

$$\frac{du}{dy} = \frac{\tau}{\mu} = \frac{\tau}{\rho\nu} = const. \tag{6}$$

Integrating this with respect to y gives

$$u(y) = \frac{\tau}{\mu}y + C = \frac{\tau}{\rho\nu}y + C \tag{7}$$

Assuming a boundary condition of $u(0) = 0$ at the plate surface, the constant C becomes 0 and yields

$$u_{\mathrm{k}} = \frac{\tau}{\mu}y = \frac{\tau}{\rho\nu}y \tag{8}$$

Fig. 2 is a schematic of the interference fringes generated in the wedge-shaped oil film. In this figure, S_k, u_k, and h_k denote the wavelength, the shear velocity, and the oil height at the k-th fringe, respectively. The oil film spreads downstream due to the shear stress τ, and the wedge angle becomes smaller. Assuming the shear stress τ does not vary locally, the difference between velocities of adjacent fringes is proportional to the reduction in wedge angle. Hence, the temporal change in fringe wavelength is expressed using equation (5) as follows [3]:

$$\frac{dS_k}{dt} = u_k - u_{k-1} = \frac{\tau}{\rho\nu}(h_{\mathrm{k}} - h_{k-1}) = \frac{\tau}{\rho\nu}\Delta h \tag{9}$$

Substituting equation (4) into equation (9) and solving for the shear stress τ yields

$$\tau = \frac{2\rho\nu\sqrt{n_{\mathrm{oil}}^2 - \sin^2\alpha}}{\lambda_0}\frac{dS}{dt} \tag{10}$$

The shear stress τ can be obtained from the temporal change in fringe wavelength dS/dt.

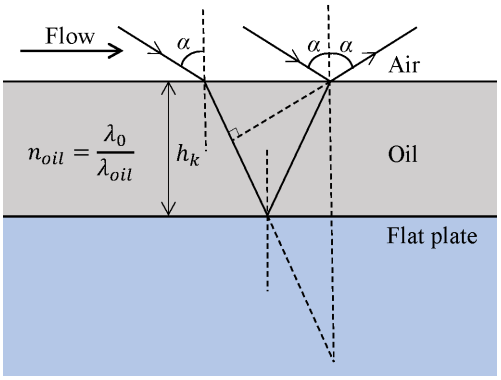

Fig. 1 Optical path difference. Light reflected from the surface of the oil and light that passes through the oil and reflects from the surface of the flat plate interfere with each other, resulting in alternating bright and dark lines.

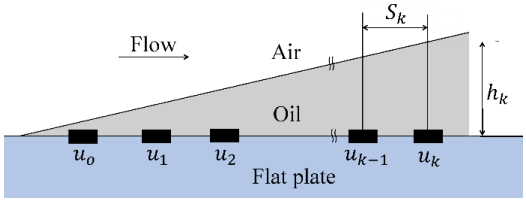

Fig. 2 Fringe pattern of oil film. The oil film spreads downstream due to the shear stress τ and becomes wedge-shaped.

3. EXPERIMENTAL SETUP

The experimental procedure is described as follows. Figures 3 and 4 show the side and top views of the measurement section, respectively. A small amount of oil is dropped at a point approximately 10 mm away from the jet impingement location on the flat plate. The oil used in this experiment has a kinematic viscosity of $\nu = 1000$ mm²/s. The nozzle is positioned perpendicular to the flat plate, at a height h of approximately 5 mm or 10 mm. The camera is fixed on a tripod at an angle of $\alpha = 30°$ with respect to the vertical direction. The camera is set to a shutter speed of 1/200 s, an aperture value of F9, an ISO sensitivity of 250, and has a pixel count of 4000 × 6000. For calibration of the interference fringes, a sheet of graph paper is placed on the measurement plate and photographed before the experiment.

The nozzle has an inner diameter of 2 mm, and the nozzle-pressure ratio p_0/p_a, where p_0 is the supply pressure and p_a the atmospheric pressure, is adjusted to 2.0, 2.5, and 3.0. Compressed air supplied from a compressor is ejected through the nozzle and impinges

on the flat plate. Interference fringes are generated in the thinned oil film using light emitted from a sodium lamp. These fringes are recorded for 500 seconds using time-lapse photography at 1-second intervals.

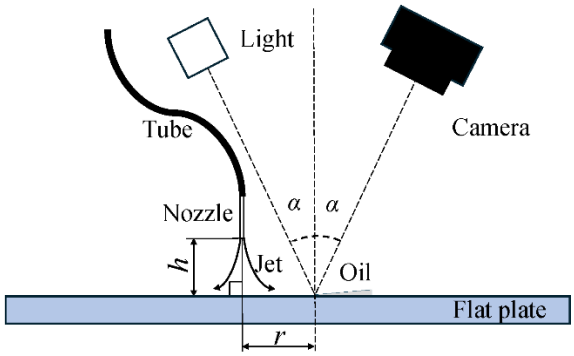

Fig. 3 Side view of experimental equipment. The experiment is conducted at different values of h and p_0/p_a.

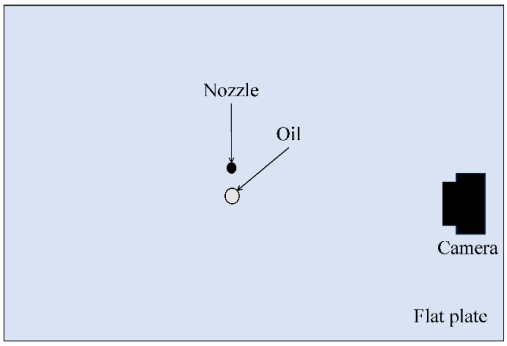

Fig. 4 Top view of experimental equipment. Oil is dropped at a position approximately 10 mm away from the jet impingement point.

4. RESULTS AND DISCUSSION

Figs. 5 (a) and 5 (b) present photographs taken at 0 s and 500 s, respectively, after the start of the measurement at a nozzle-to-plate distance $h = 5$ mm and a nozzle pressure ratio $p_0/p_a = 2.5$. The nozzle is positioned in the upper right corner of each image, and an oil droplet is placed near the nozzle. A reflection of the nozzle can also be seen in the lower right. In these photographs, the oil film can be clearly seen elongating as the jet impinges on the plate and the resulting wall jet spreads radially on the plate surface.

Figs. 6 (a) to 6 (d) are the interference fringes that appear in the oil film as shown in Fig. 5, and these are images captured from 100 s to 400 s after the start of the measurement. Each image was cropped from the analysis region indicated in Fig. 5, with a width of 64 pixels (1.0 mm) and a height of 512 pixels (8.0 mm), and then binarized. In these images the flow direction is from right to left, and the fringe spacing narrows in the downstream (leftward) direction. At 100 s, well-defined fringes have not yet appeared on the left side of the image, indicating that the downstream oil film has not thinned sufficiently to produce interference. As time goes, the fringe clearly appears on the left side, and the fringe spacing on the right side becomes larger than that on the left side. This indicates the local variation of the shear stress, i.e., the shear stress decreases downstream.

Fig. 7 presents a three-dimensional visualization of the temporal evolution of interference-fringe wavelength at positions measured from the right edge of Fig. 6. The wavelength increases as time progresses, and the further away from the jet impingement point, the smaller the ratio of wavelength to time.

Fig. 8 shows the temporal variation of the fringe wavelength S at radial distances $r = 13$ mm, 14 mm, 15 mm, and 16 mm from the jet impingement point under the same conditions ($h = 5$ mm, $p_0/p_a = 2.5$). The wavelength at each r was obtained by averaging over 129 pixels in the neighborhood and is proportional to the elapsed time. The value of dS/dt gradually decreases as r increases.

The temporal derivative dS/dt of the fringe wavelength was used to derive the shear stress distribution. Figs. 9 and 10 show the variation of the shear stress τ with the radial distance r from the jet impingement point for nozzle-to-plate distances $h = 5$ mm and 10 mm, respectively. A higher pressure ratio yields larger τ values, and τ decreases inversely proportional to r. Comparing the results at two nozzle heights, the shear stress for $h = 10$ mm is consistently slightly lower than for $h = 5$ mm. These results agree with our intuitive notion that the higher the supply pressure and the closer the nozzle is to the plate, the higher the shear stress near the jet impingement point.

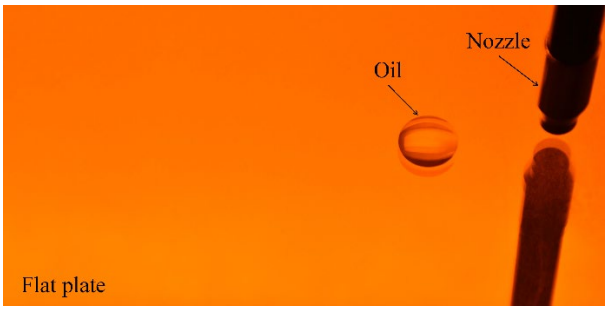

(a) $t = 0$ s.

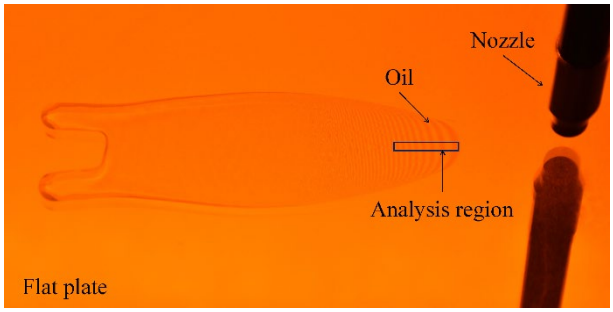

(b) $t = 500$ s.

Fig. 5 Images of oil on a flat plate. Oil on the flat plate spreads downstream as the jet impinges on the plate. The analysis is conducted within the area indicated in the figure.

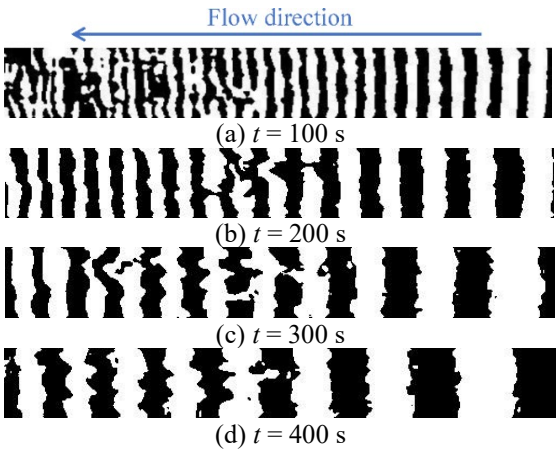

Fig. 6 Images of interference fringes. As time progresses, the wavelength of the interference fringes increases. In addition, the wavelength on the downstream side is smaller than that on the upstream side.

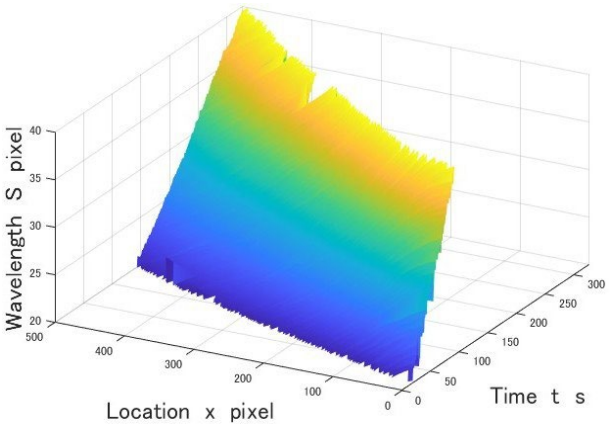

Fig. 7 Temporal evolution of interference-fringe wavelength at positions measured from the right edge of Fig. 6. The farther the distance from the jet impingement point, the smaller the value of *dS/dt* becomes.

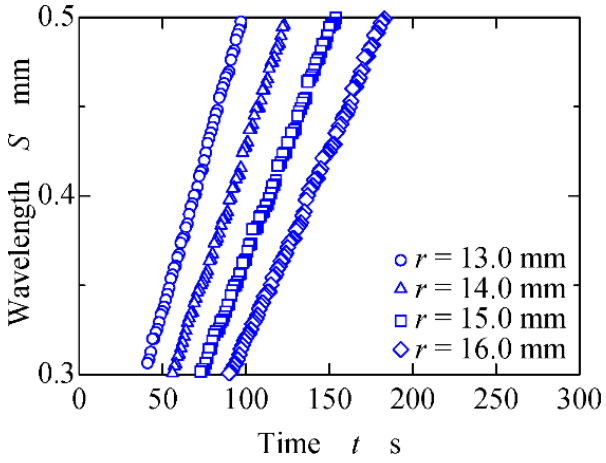

Fig. 8 Variation of wavelength with the elapsed time. The wavelength S of the interference fringes is proportional to the time.

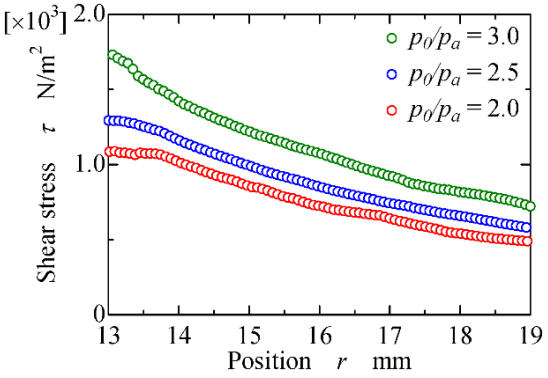

Fig. 9 Relation between τ and r at h = 5 mm. The shear stress gradually decreases as the position r increases and takes larger values at higher pressure ratio.

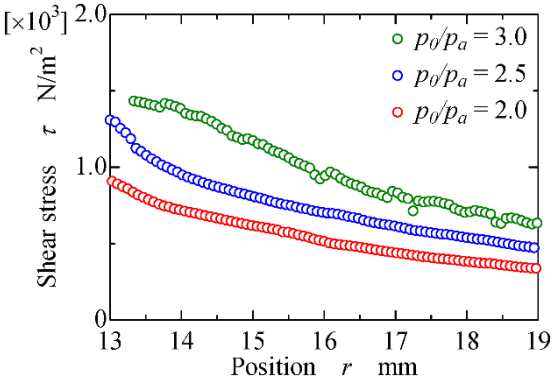

Fig. 10 Relation between τ and r at h=10 mm. Compared to the case where h = 5 mm, the shear stress is slightly lower.

5. CONCLUSIONS

Using the Oil-Film Interferometry method, the shear stress generated by a jet impinging on a flat plate was measured, and the following conclusions were drawn.

- It was shown that the shear stress due to the supersonic jet impingement on a flat plate could be measured using Oil-Film Interferometry.
- The shear stress increased with higher pressure ratios and shorter nozzle-to-plate distance.
- The shear stress decreased inversely proportional to distance from the jet impinging point.

REFERENCES

[1] L. H. Tanner and L. G Blows, A study of the motion of oil films on surfaces in air flow, with application to the measurement of skin friction, *J. Phys. E.* Vol. 2, No. 3, pp. 194-202, 1976.

[2] T. Imai, K. Kondo, Y. Suzuki and Y. Miki, Measurement of wall shear stress on an airfoil surface by using the oil film interferometry with PIV analysis applied to Fizeau fringes, *Bulletin of the JSME*, Vol. 18, No. 1, pp. 1-18, 2023.

[3] Y. Tsuji, A. Ido, and M. Nishioka, Universality of Mean Velocity Profile in High Re-Number Turbulent Boundary Layer, *Transactions of the JSME,* Vol. 87, pp. 1-24, 2021.